JOURNAL OF MATERIALS SCIENCE **34** (1999) 3221–3239

Natural rubber/epoxidised natural rubber-25 blends: morphology, transport phenomena and mechanical properties

T. JOHNSON, SABU THOMAS*
School of Chemical Sciences, Mahatma Gandhi University, Priyadarshini Hills P. O., Kottayam—686 560, Kerala, India

Blends of natural rubber (NR)/epoxidised natural rubber (ENR) were prepared and their morphology, transport behaviour and mechanical properties have been studied. Ebonite method was used to study the blend morphology. Transport behaviour of pentane, hexane, heptane and octane was studied in the temperature range 27–60 °C. Different transport parameters such as rate constant, diffusion and permeation coefficients, and sorption coefficient have been calculated. Temperature dependence of diffusion has been used to estimate the activation parameters. The improved performance of NR/ENR blends has been established from the mechanical studies of unswollen, swollen and deswollen samples.

1. Introduction

The transport properties of polymer blends are of interest for the practical application of blends in air retention, vapour resistance, permselectivity etc. as well as for the insight into the morphology of the blend that can be gained from study of the penetration of small molecules into the structure. Mesrobian and Ammondson [1] reported the permeability of *n*-heptane, methyl salicylate and methyl alcohol through polyethylene-nylon blends. Cates and White [2–4] were among the first to report the sorption behaviour of water in blends of polyacrylonitrile/cellulose, polyacrylonitrile/silk and polyacrylonitrile/cellulose acetate. The sorption of water in PAN-cellulose acetate and PAN-cellulose varied linearly with blend composition. However, in the case of PAN-silk blend, a complicated sorption behaviour was obtained.

Saltonstall and co-workers [5] have reported the desalination of sea water through membranes from blends of cellulose triacetate and cellulose diacetate. Shchori and Jagur-Grodzinski [6] have described the permselective properties of blends of poly(vinyl pyrrolidone) (PVP) and a crown ether copolymer. Molecular transport of haloalkanes through blends of ethylene-propylene copolymer and isotactic polypropylene has been studied by Aminabhavi and Phayde [7]. Aminabhavi and co-workers [8] have reported the sorption of aliphatic esters through tetrafluoroethylene/propylene copolymeric membranes. The results show that diffusion coefficients, permeation coefficients and kinetic rate constants decrease with increase in the size of esters. It was found that the structural characteristics of the penetrant molecules also play an important role in the molecular transport.

The sorption kinetics and equilibria of some normal alkanes namely hexane in solution cast blend films of atactic polystyrene (PS) and poly(2,6-dimethyl-1,4-phenylene oxide) (PPO) have been studied extensively by Hopfenberg and co-workers [9–11]. The effects of temperature, penetrant activity, blend composition and thermal history on the sorption kinetics and equilibria of *n*-hexane in the PS-PPO blends have been studied.

Gregor *et al.* [12–14] described the synthesis and properties of ion-selective membranes prepared from a polyelectrolyte compound and an uncharged, second polymeric component. These studies include the blends of poly(styrene sulphonic acid) and a copolymer of acrylonitrile and vinyl chloride. The most extensive study of the permeability of rubber blends was the early work of Barrer [15]. To our knowledge, till date no studies have been reported on the morphology and transport characteristics of NR/ENR blend membranes. The main objective of the present study is a detailed investigation of morphology, transport properties and mechanical behaviour of natural rubber/epoxidised natural rubber blend membranes.

2. Experimental

Indian standard natural rubber (ISNR-5) was supplied by RRII, Kottayam, India. Epoxidised natural rubber (ENR) epoxyprene with 25 mol % epoxidation was supplied by Rubber Research Institute, Malaysia. The number average molecular weight of NR and ENR is in the range 1×10^6 to 9.9×10^5. Compounding was done on a two-roll mixing mill (Friction ratio 1 : 1.4), according to ASTM D15-627. The basic formulation used is given in Table I. Natural rubber/epoxidised natural rubber

* Author to whom all correspondence should be addressed.

TABLE I Compounding recipe (parts per hundred parts of rubber by weight)

Ingredients	NR	ENR-25
ZnO	5	5
Stearic acid	2	2
Calcium stearate	0	3
CBS[a]	1.5	1.5
Sulphur	2.5	1.5
TDQ[b]	1	1

[a] *N*-cyclohexyl-2-benzothiazyl sulphenamide.
[b] Trimethyl dihydro quinoline.

blends were prepared by the masterbatch technique. The blend compositions are 70/30, 50/50 and 30/70. The compounds were then compression moulded along the mill grain direction using an electrically heated hydraulic press at 150 °C.

2.1. Morphology

The most widely used method for studying the morphology of elastomer blends is the ebonite method [16], in which the preferential reaction of one of the rubber phases with sulphur and zinc oxide effects a large increase in its electron density. The reaction medium for the ebonite treatment consists of molten sulphur/accelerator (*N*-cyclohexyl-2-benzothiazyl sulphenamide)/zinc stearate in the weight ratio 90/5/5. Small pieces of the samples are cut and are immersed in the molten sulphur mixture for 8 h at 120 °C. The excess sulphur was carefully scrapped off from the outer surface before thin sections were cut for SEM observations using a JEOL-JSM-35C model scanning electron microscope. The dimensions of the dispersed phase were calculated from the SEM photomicrographs by considering more than 300 domains.

2.2. Swelling experiment

Circular samples of diameter 1.9 cm were cut from vulcanised sheets and soaked in solvents (15–20 ml) taken in test bottles kept at constant temperature in an air oven. The samples were weighted at periodic intervals in an electronic balance (Shimadzu, Libror AEU-210, Japan) that measured reproducibly within ±0.0001 g. The weighings were continued till equilibrium swelling was attained.

2.3. Physico-mechanical testings

The mechanical testings were carried out using a universal testing machine (UTM) at 27 °C with a crosshead speed of 500 mm/min using dumbbell shaped tensile specimens according to ASTM D 0412-80. These experiments were carried out for unswollen, swollen and deswollen samples.

3. Results and discussion

3.1. Cure characteristics

The rheographs of the mixes are given in Fig. 1 and cure characteristics in Table II. The minimum torque in the rheograph is presented as minimum viscosity (M_L)

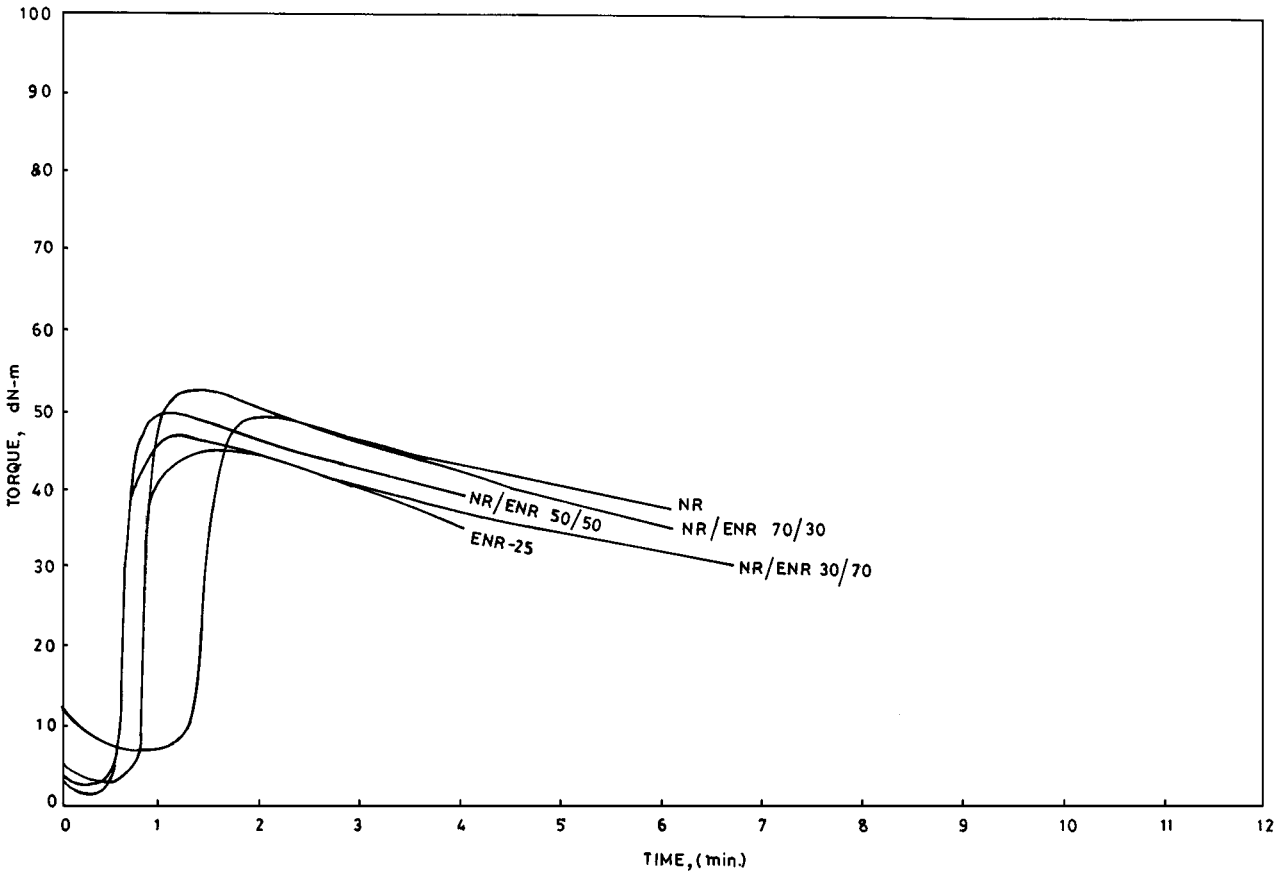

Figure 1 Rheograph of the mixes.

TABLE II Cure characteristics

Sample	M_L (dN-m)	M_H (dN-m)	t_2 (m:s)	t_1 (m:s)	t_{90} (m:s)	CRI (min^{-1})
NR	7.5	50	6	5.5	8.25	44.44
NR/ENR 70/30	3.5	53.5	3.5	3.25	5	66.66
NR/ENR 50/50	1.5	50	2.5	2.25	4	66.66
NR/ENR 30/70	2.75	47	2.75	2.5	4	80
ENR-25	3.5	45.5	3.5	3.25	4.5	100

TABLE III Blend characteristics

Characteristics	NR/ENR 70/30	NR/ENR 30/70
$\bar{D}_n$ (μm)	7.70	4.116
$\bar{D}_w$ (μm)	11	5.32
$\bar{D}_a$ (μm)	9.25	4.68
$\bar{D}_v$ (μm)	10.725	5.38
PDI	1.43	1.29

value and is a measure of the extent of mastication. The low M_L value of 50/50 composition indicates its higher extent of mastication during mixing. The maximum torque in the rheograph is presented as maximum viscosity M_H. Values are higher and comparable for NR, 70/30 and 50/50.

The induction time t_1 determined from the rheograph is the time taken to start vulcanisation process. It is clear from the data that the vulcanisation of 50/50 blend starts first. This may be due to a fine dispersion of compounding ingredients in 50/50 blend. The rheometric scorch time, t_2 (premature vulcanisation time) is the time taken for minimum torque value to increase by two units. Pure NR mix shows maximum scorch safety while 50/50 blend is scorchy. Optimum cure time (t_{90}) is the vulcanisation time to get optimum physical properties and is calculated using the equation

$$T_{90} = (M_H - M_L) \times .9 + M_L \tag{1}$$

where T_{90} is the optimum cure torque. Optimum cure time t_{90} is the time corresponding to optimum cure torque. NR takes maximum cure time while NR/ENR 50/50, ENR-25 and NR/ENR 30/70 show comparatively lower values.

Cure rate index (CRI) is calculated using the equation [17]

$$\text{CRI} = 100/t_{90} - t_2 \tag{2}$$

The higher the CRI values, the higher the vulcanisation rate. From Table II it can be seen that ENR-25 has the highest cure rate and NR the minimum. The cure activating component is ENR and therefore 30/70 composition has the highest cure rate among the blend compositions.

3.2. Morphology

The morphologies of NR, ENR-25 and their different blend compositions are presented in Fig. 2a–e. Fig. 2a is the morphology of ebonite treated NR samples. This presents a smooth, simple phase morphology with tiny debonded particles of NR, which occurs at the time of cryobreaking. Fig. 2b represents the morphology of ENR-25 sample. It is clear from the figure that the highly crosslinked gel phase [18, 19] exist as separate entity. The debonding phenomena observed in NR is absent here.

The morphologies of the blend compositions are presented in Fig. 2c–e. The tiny holes observed in the figure comes from the debonding of dispersed phase from the continuous phase. As already established by Roland and Böhm [20] and Tokita [21], that during mixing of rubber blends, the dispersed domains are deformed during the passage through the high shear regions of the mixing mill and under such conditions the domains will undergo break-up to form smaller particles or coalesce to form larger dispersed domains. In fact the final morphology is an equilibration between domain break-up and coalescence. The morphologies presented proves this to be the case in NR/ENR blends (Fig. 3a and b). The size characteristics of the dispersed phase ($\bar{D}_n$, $\bar{D}_w$, $\bar{D}_a$ and $\bar{D}_v$) and its distribution (polydispersity index values) of the different blend compositions are presented in Table III. These are calculated using the equations [22];

No. average diameter,

$$D_n = \frac{\Sigma N_i D_i}{\Sigma N_i} \tag{3a}$$

Weight average diameter,

$$D_w = \frac{\Sigma N_i D_i^2}{\Sigma N_i D_i} \tag{3b}$$

Surface area average diameter,

$$D_a = \frac{\Sigma N_i D_i^2}{2\sqrt{\Sigma N_i}} \tag{3c}$$

Volume average diameter,

$$D_v = \frac{\Sigma N_i D_i^3}{3\sqrt{\Sigma N_i}} \tag{3d}$$

where N_i is the number of particles having a diameter D_i.

Poly dispersity index (PDI) which is a direct measure of size distribution of the dispersed phase is calculated as

$$\text{PDI} = D_w/D_n \tag{4}$$

It is clear from the table that $\bar{D}_n$, $\bar{D}_w$, $\bar{D}_a$ and $\bar{D}_v$ decrease as the composition changes from NR/ENR 70/30 to NR/ENR 30/70. NR/ENR 50/50 composition shows a co-continuous morphology. The PDI values show more uniform particle distribution for 30/70. The normal and the cumulative distribution curves of NR/ENR 70/30 and NR/ENR 30/70 blend compositions given in Fig. 4 also show the particle size distribution for these blends.

3.3. Transport properties

3.3.1. Effect of blend composition

The change in hexane uptake with blend composition is depicted in Fig. 5. NR shows the maximum solvent

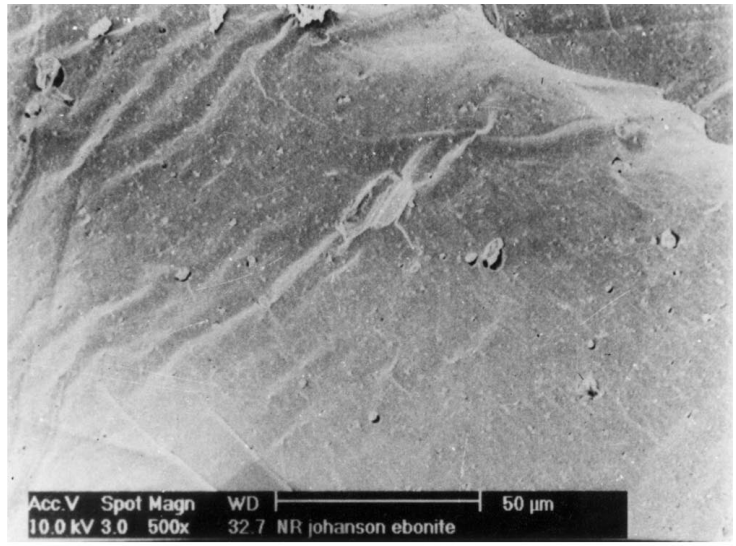

(a)

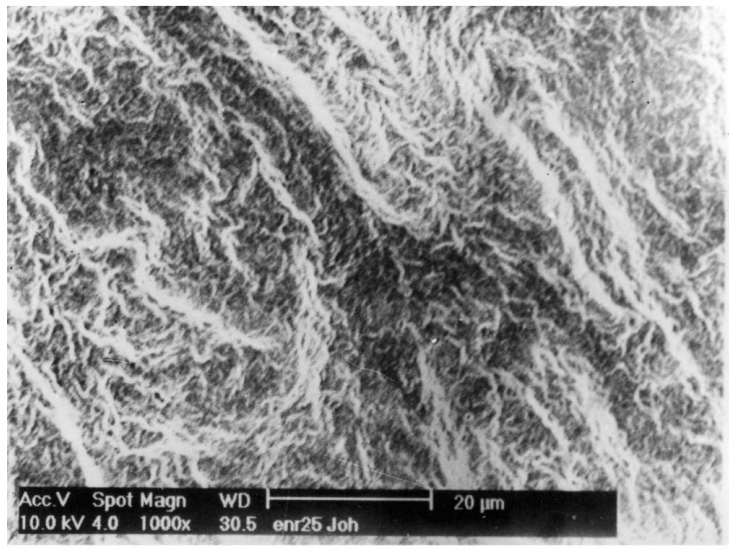

(b)

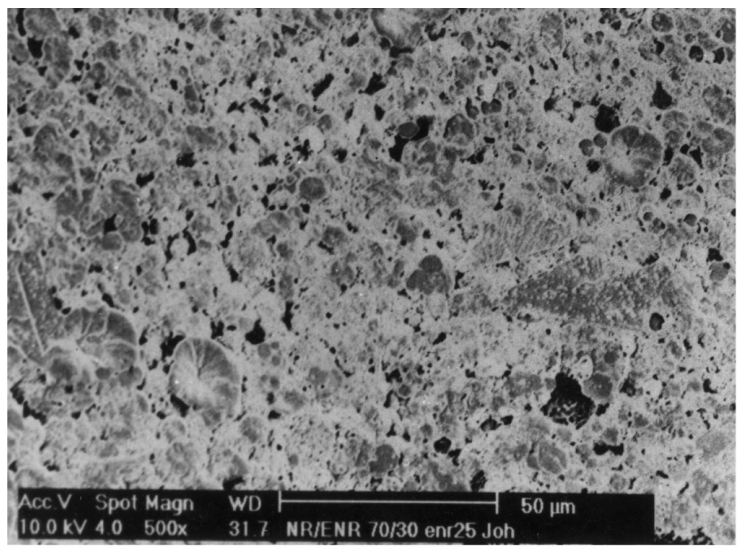

(c)

Figure 2 SEM Photographs of (a) NR (b) ENR-25 (c) NR/ENR 70/30 (d) NR/ENR 50/50 and (e) NR/ENR 30/70. (*Continued*.)

uptake and ENR-25 the minimum. The maximum solvent uptake decreases with increase in volume fraction of ENR-25. The inherent solvent resistance of ENR-25 may be the reason for the observed solvent uptake behaviour. The chemical structures of NR and ENR are given in Fig. 6. The epoxy group hinders the chain flexibility with a consequent increase in T_g value (T_g of NR $-72\,^{\circ}C$ and ENR-25 $-47\,^{\circ}C$). Also the polar nature of

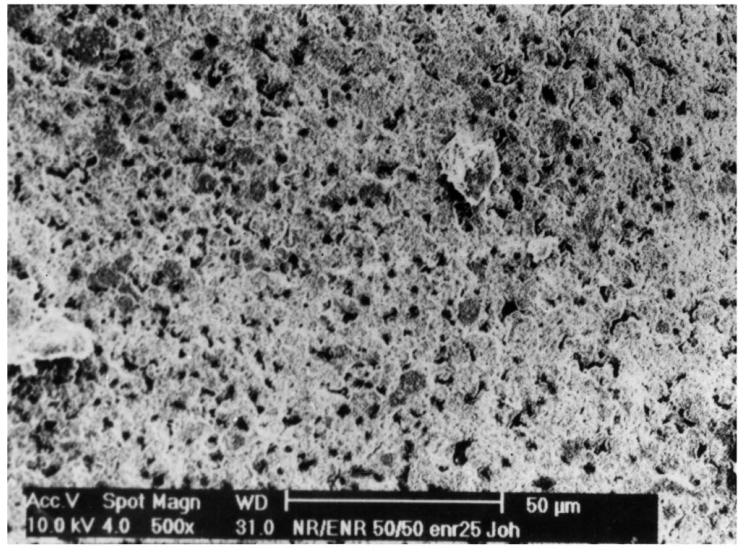

(d)

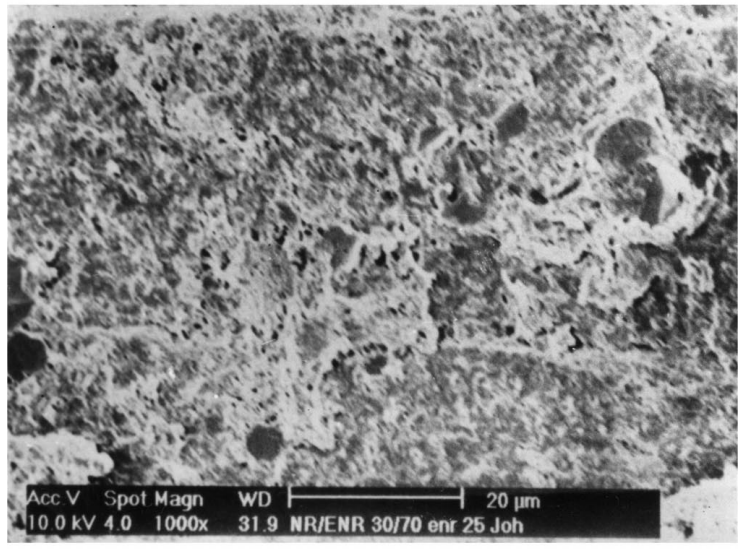

(e)

Figure 2 (*Continued*.)

ENR chains increases the interchain interaction and this factor also contributes to the decreased chain flexibility. It is established that the permeability of heterogeneous rubber-rubber blends is intermediate between that of the components [23]. The observed solvent uptake is in accordance with this observation.

The solvent uptake with increasing penetrant size for 50/50 composition is shown in Fig. 7. The Q_∞ values increase with increasing penetrant size from pentane to heptane and decreases for octane. This observation can be explained on the basis of the solubility parameter difference between the polymer and penetrant. The difference in the solubility parameters between the polymer and the penetrant is often used to characterise the sorption behaviour of the penetrant in the polymer membrane [24, 25]. The solubility of the penetrant generally becomes high when the difference in the solubility parameters between the polymer and the penetrant is small. The solubility parameter differences for different polymer solvent systems are given in Table IV. Though this value is lowest for octane, the lowest uptake for octane is due to its larger size compared to pentane, hexane and heptane. For the other three solvents, the uptake is in accordance with the solubility parameter difference.

TABLE IV Solubility parameter difference between polymer and solvent (kJ/mol)

Solvent	NR	NR/ENR 70/30	NR/ENR 50/50	NR/ENR 30/70	ENR
Pentane	1.9	2.26	2.5	2.74	3.1
Hexane	1.5	1.86	2.1	2.34	2.7
Heptane	1.1	1.46	1.8	1.94	2.3
Octane	0.7	1.06	1.3	1.54	1.9

3.3.2. Diffusivity

The dynamic swelling properties of a polymer film include the solvent sorption rate, the rate of approach to equilibrium swelling, the solvent front velocity and the transport mechanism controlling solvent sorption. For a Fickian mechanism, the rate of approach to equilibrium can be characterised by a diffusion coefficient. For

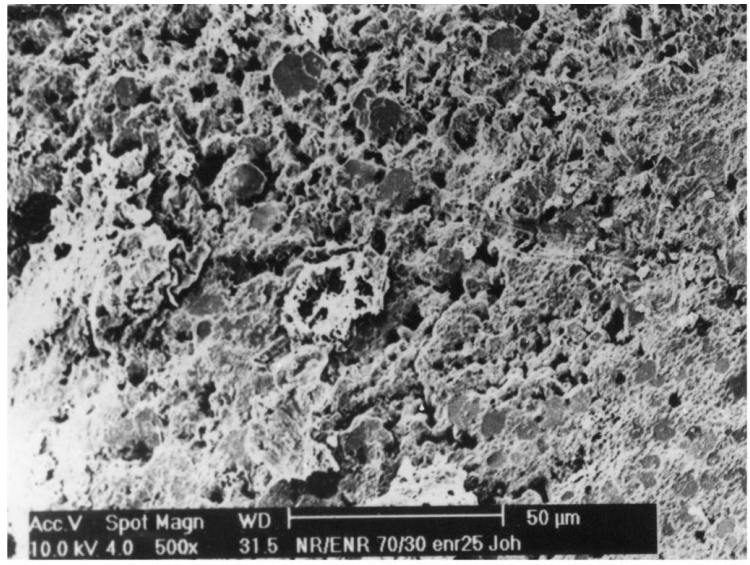

(a)

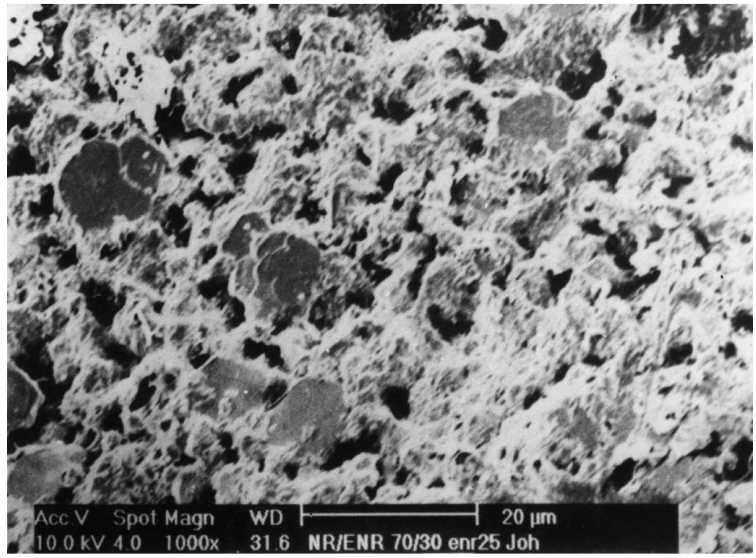

(b)

Figure 3 Surface morphology of 70/30 composition (a) 500 magnification and (b) 1000 magnification.

ordinary diffusion, Fick's law is the appropriate constitutive equation for the mass transfer flux and a mutual diffusion coefficient can be defined [26, 27]. For a plane geometry of the polymer sheet, the diffusion coefficient D, can be calculated from [28]

$$Q_t/Q_\infty = 1 - \sum_{n=0}^{\infty} \left[(8/(2n+1)^2\pi^2)\, e^{(2n+1)^2\pi^2(D_t/h^2)}\right] \tag{5}$$

where t is the time and h is the initial thickness of the polymer sheet. Although this equation can be solved readily, it is instructive to examine the short-time limiting expression as well [28]

$$Q_t/Q_\infty = [4/\pi^{1/2}]\left[D_t/h^2\right]^{1/2} \tag{6}$$

From a plot of Q_t vs. $t^{1/2}$, a single master curve is obtained which is initially linear. Thus, D can be calculated from a rearrangement of Equation 6 [29, 30] as

$$D = \pi[h\theta/4Q_\infty]^2 \tag{7}$$

where θ is the slope of the initial linear part of the graph of Q_t vs. $t^{1/2}$.

The diffusion coefficient values derived from Equation 7 are compiled in Table VI. The variation of D value with volume fraction of NR is given in Fig. 8. The diffusion coefficient values of the blends are found to be intermediate between that of the components. The values presented in the table show that the diffusion coefficient values increase with temperature and decrease with penetrant size.

The solubility or the sorption of the penetrant molecule is also an important parameter as far as the permeation of a penetrant molecule into a polymer matrix is concerned. Sorption describes the initial penetration and dispersal of permeant molecules into the polymer matrix. Sorption coefficient (S) is obtained from the following equation [29]

$$S = M_\infty/M_0 \tag{8}$$

The variation of sorption coefficient with temperature and penetrant size is given in Table V. The value

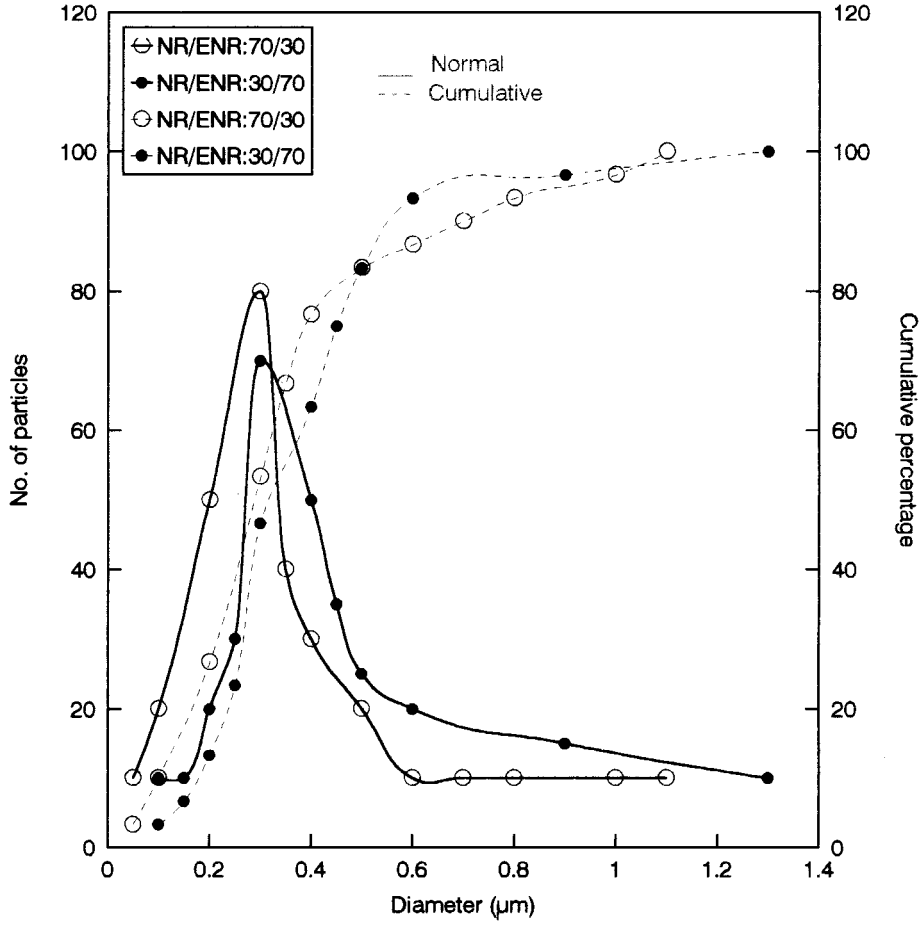

Figure 4 Particle size distribution for NR/ENR 70/30 and NR/ENR 30/70 compositions.

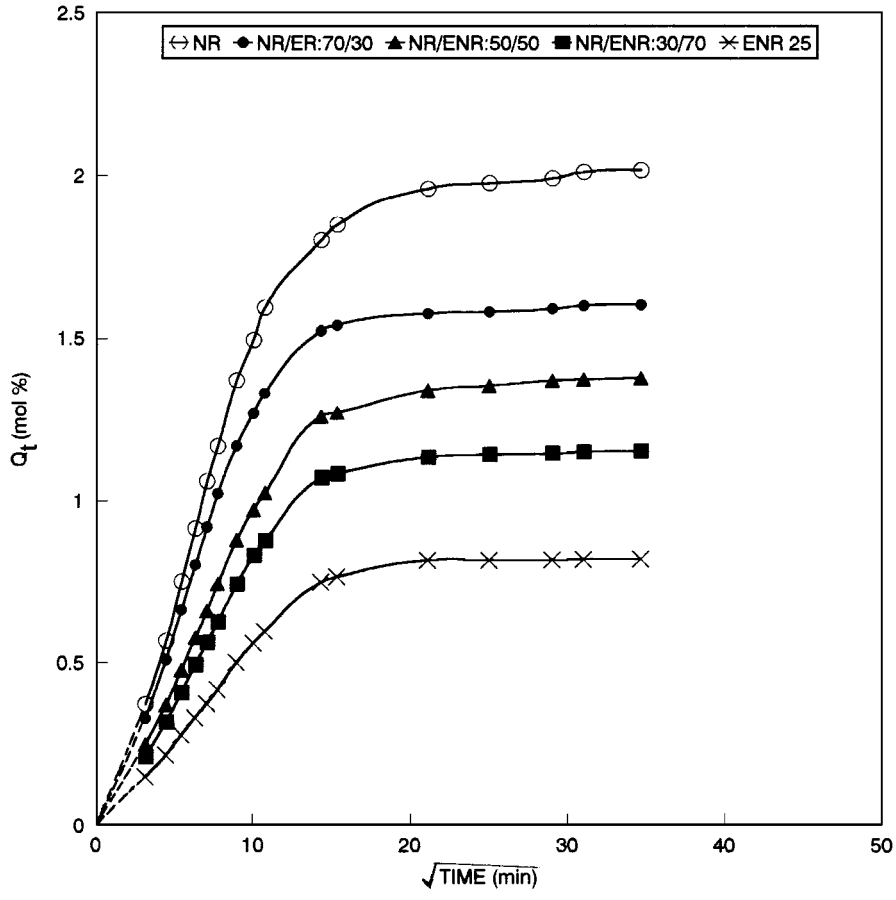

Figure 5 Mol % uptake of individual components and blend compositions in hexane.

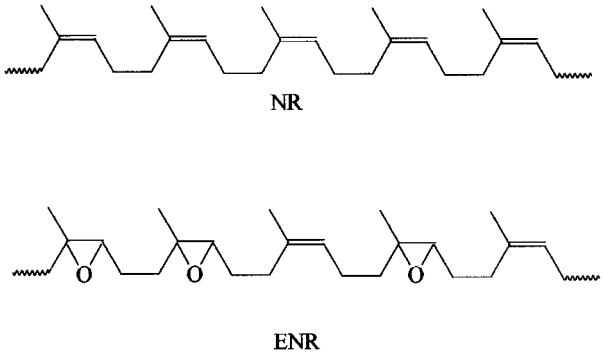

Figure 6 Structure of NR and ENR.

decreases with temperature for NR whereas it increases for blend composition and ENR-25. This may be attributed to the negative heat of sorption for NR. But the sorption coefficient values increase with increase in penetrant size up to heptane but decrease for octane.

The permeability data, as calculated from the simple empirical relation

$$P = DS \tag{9}$$

given in Table V follow nearly the same pattern as those of diffusivities. This simple relation holds for the permeation process when D obeys Fick's diffusion law and S obeys Henry's law [31]. For the penetrant polymer systems used in this study, it is not certain to what degree one or both laws are obeyed. Thus, the P values presented in Table V are to be considered as estimates of the permeability coefficient.

3.3.3. Kinetics of diffusion

Swelling kinetics of polymers are important when barrier applications of polymers are considered. For polymer-solvent systems where the polymer thickness does not increase substantially, the first order rate kinetics can be applied to the diffusion-controlled swelling [32]. Thus efforts have been made to investigate the kinetics of sorption in terms of the first-order kinetic mode. From the sorption results of polymer-solvent systems, the first-order kinetic rate constants have been evaluated by using the equation

$$dc/dt = k(C_\infty - C_t) \tag{10}$$

where k is the first-order rate constant (min^{-1}). Integration of Equation 10 gives,

$$k_t = 2.303 \log[C_\infty/(C_\infty - C_t)] \tag{11}$$

Here C_t and C_∞ represent the concentrations at time t and at infinite time respectively. The values of rate constant obtained are given in Table VII. The correlation coefficient in the determination of the first order kinetic

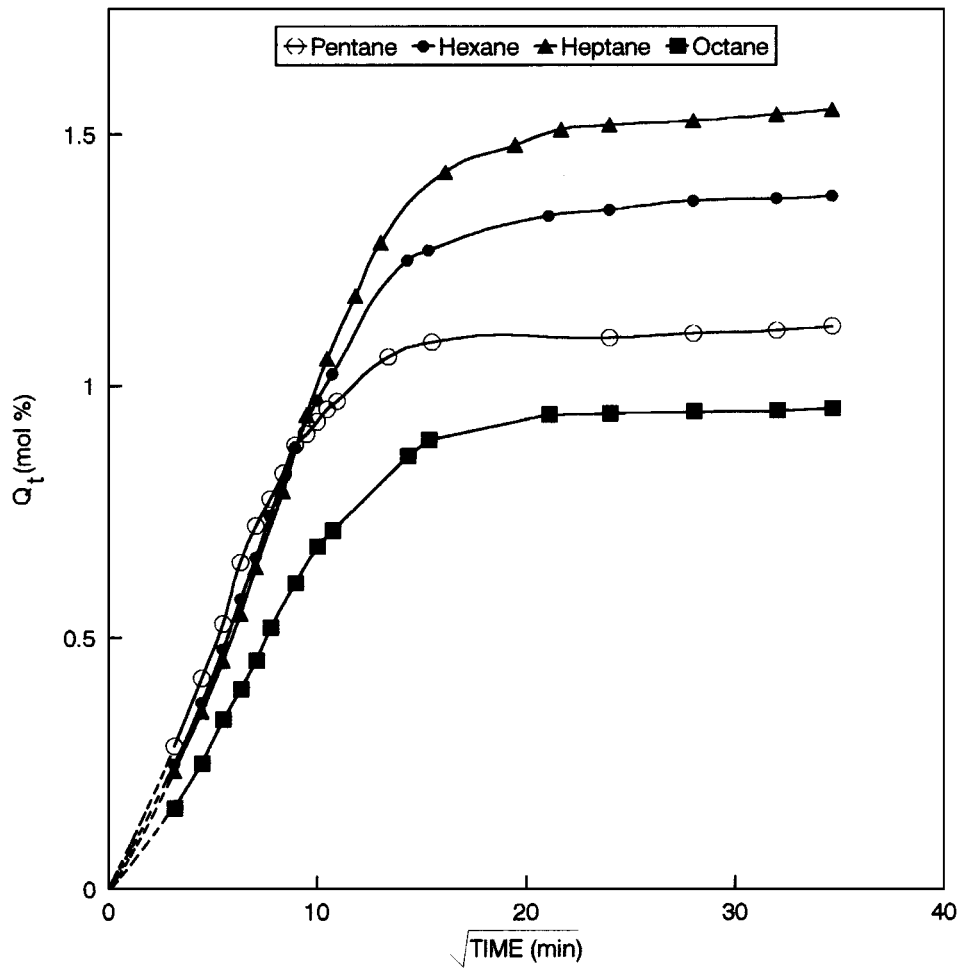

Figure 7 Mol % uptake of 50/50 composition in different solvents.

TABLE V Values of P and S

Solvent	Temperature (°C)	$P \times 10^6$ (cm^2/s) NR	NR/ENR 70/30	NR/ENR 50/50	NR/ENR 30/70	ENR	S(g-g^{-1}) NR	NR/ENR 70/30	NR/ENR 50/50	NR/ENR 30/70	ENR
Pentane	27	1.77	1.43	0.96	0.71	0.46	1.11	0.92	0.80	0.67	0.48
Hexane	27	1.50	1.3	0.81	0.68	0.38	1.73	1.38	1.18	0.99	0.70
	40	1.65	1.60	1.21	0.82	0.38	1.50	1.30	1.13	0.96	0.95
	50	1.80	1.24	1.14	0.69	0.52	1.55	1.43	1.13	1.16	0.98
	60	2.01	1.63	1.47	1.03	0.57	1.59	1.49	1.21	1.18	1.12
Heptane	27	1.73	1.17	0.78	0.63	0.37	2.13	1.74	1.55	1.38	1.06
	40	1.86	1.57	1.28	0.78	0.54	2.06	1.74	1.55	1.39	1.14
	50	2.09	1.61	1.27	0.94	0.55	1.99	1.77	1.62	1.47	1.19
	60	2.49	1.91	1.51	1.15	0.78	2.07	1.77	1.64	1.49	1.23
Octane	27	0.75	0.68	0.57	0.32	0.13	1.02	0.87	0.67	0.52	0.43
	40	0.86	0.71	0.64	0.38	0.17	1.12	0.94	0.72	0.61	0.45
	50	0.99	0.82	0.71	0.42	0.19	1.18	0.98	0.81	0.72	0.47
	60	1.09	0.91	0.84	0.51	0.26	1.24	1.04	0.92	0.81	0.52

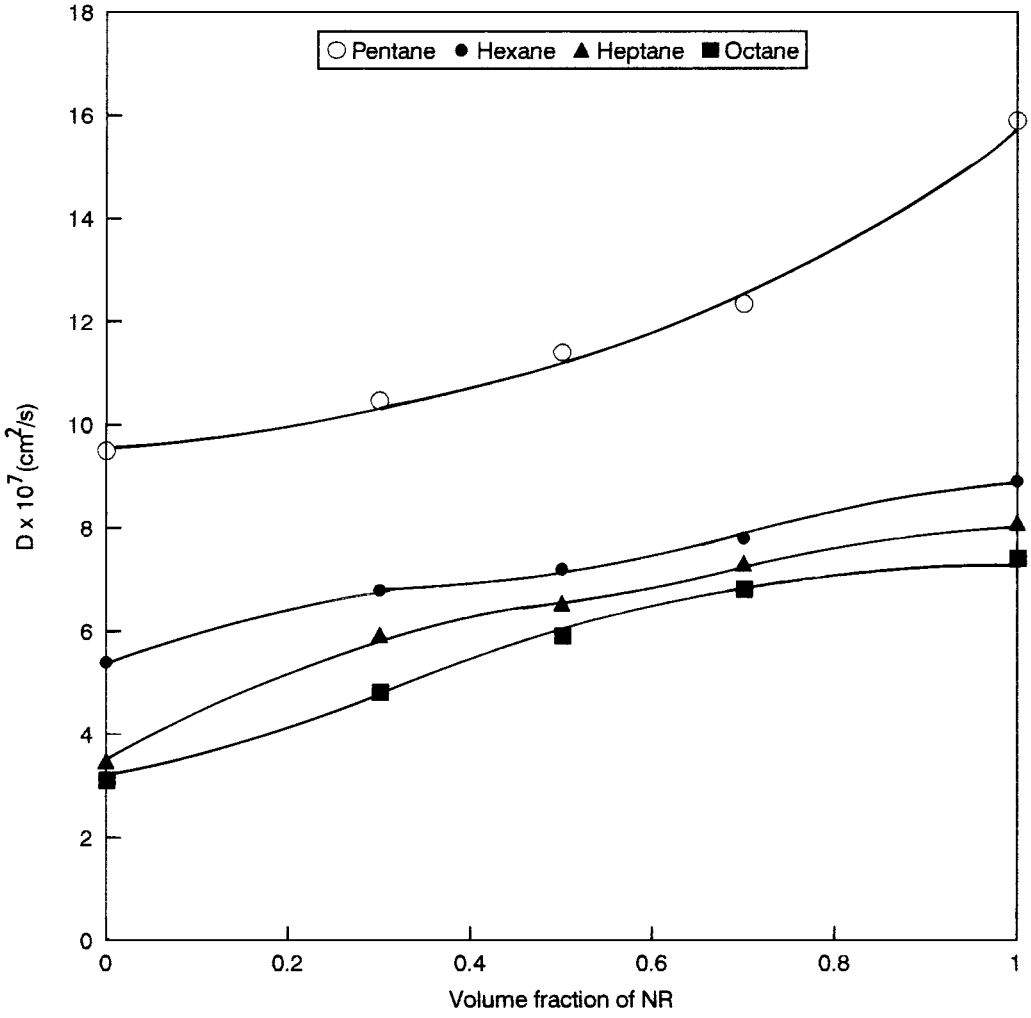

Figure 8 Variation of D with volume fraction of NR in different solvents at 27 °C.

rate constants was found to be 0.99. NR has the highest rate constant and ENR the lowest. This also indicates that the rate of uptake is highest for the NR phase and lowest for ENR. The decreased rate of uptake in ENR compared to NR is due to the decreased chain flexibility of ENR. As the temperature increases the rate constant i.e., rate of uptake increases due to the increased chain flexibility. In the case of blends, rate of solvent uptake decrease with increase in ENR fraction. The values of diffusion coefficient determined are also in agreement with that of rate constant values.

3.3.4. Temperature effects and activation parameters

To study the effect of temperature, the sorption experiments were carried out at 40, 50 and 60 °C in addition

TABLE VI Values of diffusion coefficient, $D \times 10^7$ (cm^2/s)

Solvent	Temperature (°C)	NR	NR/ENR 70/30	NR/ENR 50/50	NR/ENR 30/70	ENR
Pentane	27	15.89	12.34	11.42	10.47	9.50
Hexane	27	8.90	7.80	7.20	6.80	5.40
	40	11.81	10.91	9.62	8.21	7.10
	50	12.65	11.82	10.84	8.98	7.40
	60	13.63	12.91	11.72	9.47	7.10
Heptane	27	8.10	7.32	6.54	5.93	3.49
	40	9.47	8.72	7.82	6.12	4.84
	50	10.47	9.38	8.42	6.42	4.64
	60	12.01	11.14	9.97	8.01	6.34
Octane	27	7.40	6.80	5.90	4.80	3.10
	40	7.70	7.10	6.40	5.21	3.82
	50	8.42	7.81	6.93	5.43	4.27
	60	8.82	8.21	7.63	6.21	5.14

TABLE VII Rate constant values, $k \times 10^2$ (min^{-1})

Solvent	Temperature (°C)	NR	NR/ENR 70/30	NR/ENR 50/50	NR/ENR 30/70	ENR
Pentane	27	2.41	2.38	2.09	1.94	1.82
Hexane	27	1.30	1.55	1.13	1.16	1.03
	40	1.70	1.64	1.53	1.32	1.20
	50	1.81	2.16	1.71	1.18	1.31
	60	1.94	2.20	2.08	1.67	1.50
Heptane	27	1.37	1.16	1.01	0.96	0.69
	40	1.27	1.23	1.18	1.03	0.92
	50	1.38	1.30	1.21	1.04	0.79
	60	1.54	1.42	1.39	1.27	1.10
Octane	27	0.98	0.87	0.74	0.62	0.54
	40	1.10	0.94	0.84	0.74	0.61
	50	1.18	1.16	1.02	0.84	0.68
	60	1.21	1.18	1.14	1.01	0.74

to 27 °C. Figs 9 and 10 represent the diffusion curves of NR and ENR-25. It can be seen that the maximum solvent uptake decreases for NR whereas it increases for ENR.

It is also relevant to estimate the activation energy for diffusion E_D and that for permeation E_P from the following Arrhenius relationship [33]

$$\log X = \log X_0 - \frac{E_X}{2.303\,RT} \tag{12}$$

where X stands for either D or P. X_0 represents either D_0 or P_0 and E_X is either E_D or E_P i.e., the activation energy of the process under consideration. A representative plot of log D vs. $1/T$ is given in Fig. 11. From the slopes of the curves, the values of E_D and E_P have been estimated by the linear regression analysis and are given in Table VIII. The uncertainty in E_D and E_P values range from ± 0.001 to ± 0.003. The values are maximum for ENR which results from the high solvent resistance of ENR. The values decrease with increase

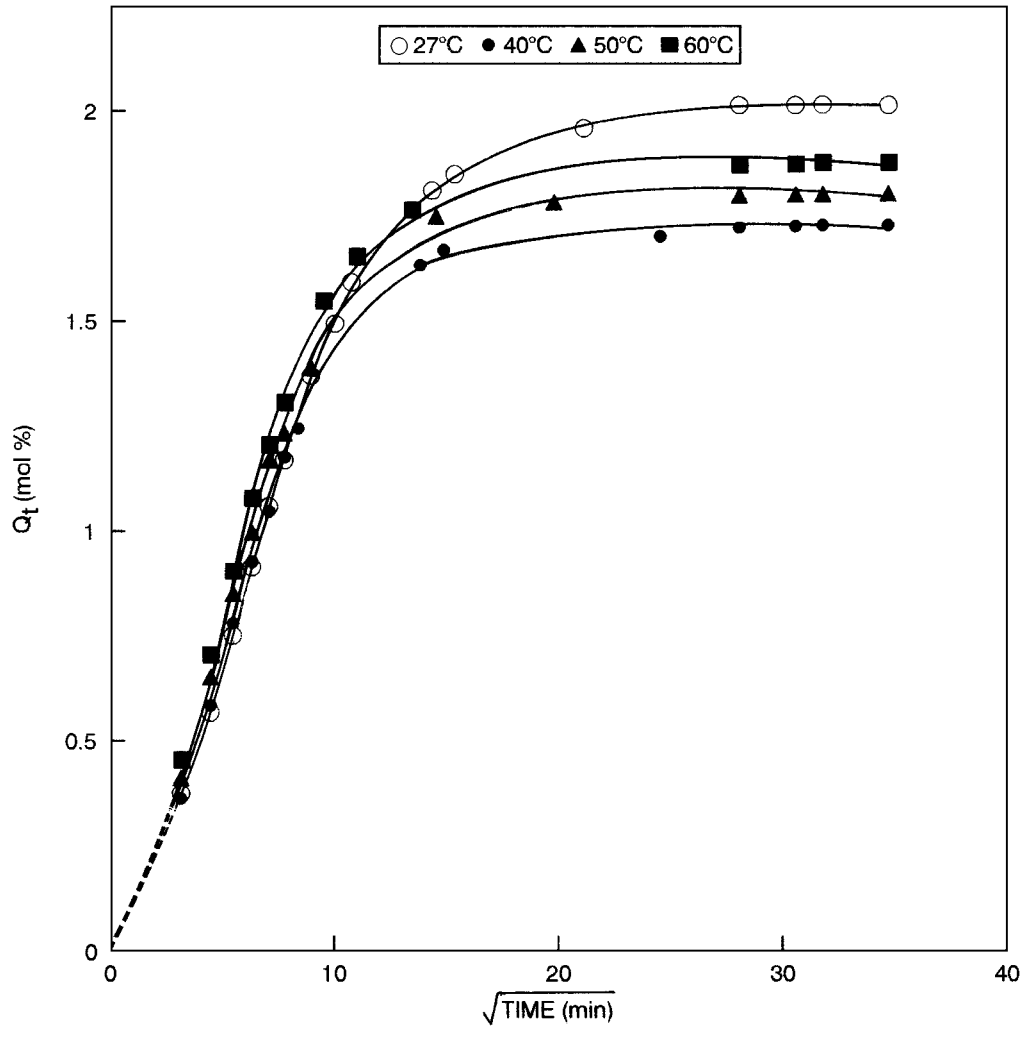

Figure 9 Effect of temperature on mol % heptane uptake in NR.

TABLE VIII Activation parameters

	E_P(kJ/mol)					E_D(kJ/mol)				
Solvent	NR	NR/ENR 70/30	NR/ENR 50/50	NR/ENR 30/70	ENR	NR	NR/ENR 70/30	NR/ENR 50/50	NR/ENR 30/70	ENR
Hexane	3.25	3.95	6.34	6.84	7.05	3.89	5.18	5.26	5.72	6.02
Heptane	4.12	5.76	7.12	7.46	7.64	4.38	4.91	5.47	5.63	6.48
Octane	4.53	6.01	6.86	7.67	7.83	4.78	5.01	5.86	6.04	6.78

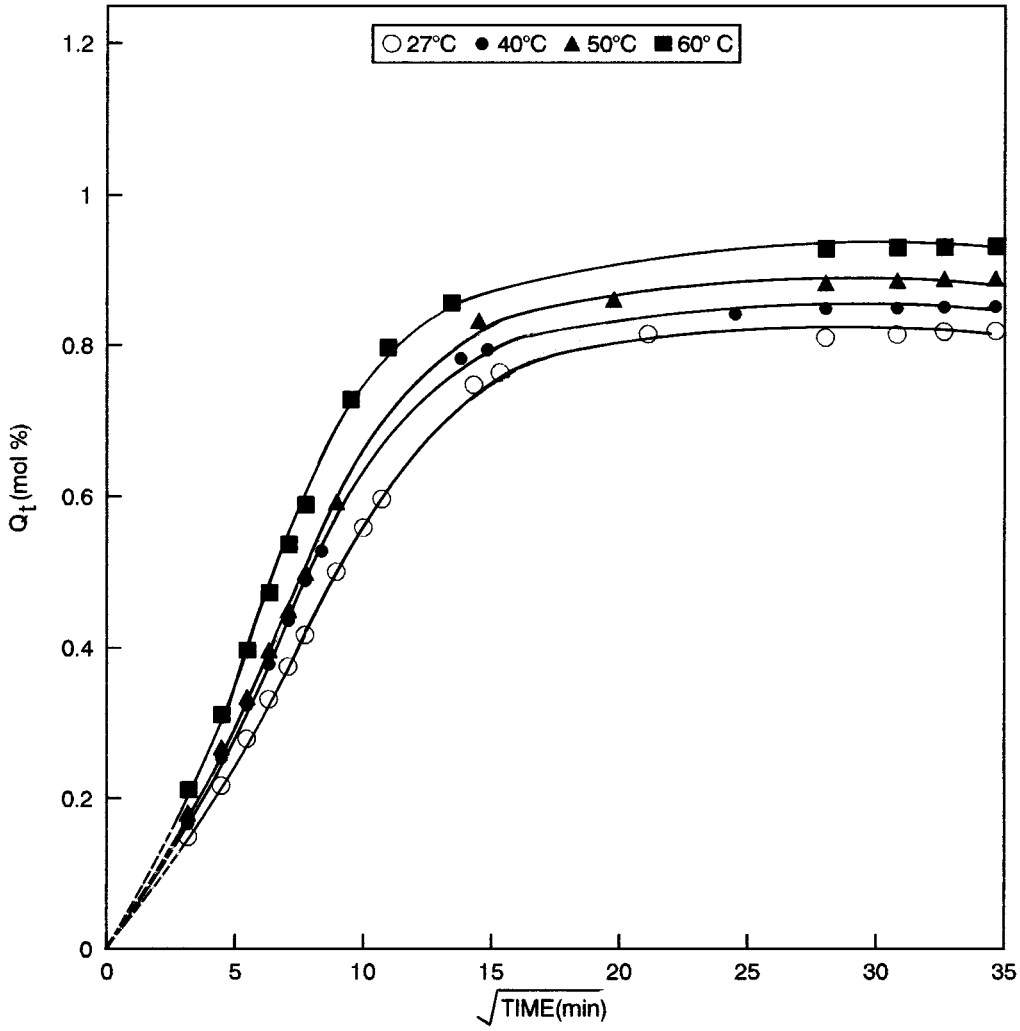

Figure 10 Effect of temperature on mol % heptane uptake in ENR-25.

in volume fraction of NR and is minimum for NR. The enthalpy of sorption is calculated using the equation

$$\Delta H_S = E_P - E_D \tag{13}$$

The ΔH_S values are tabulated in Table IX. ΔH_S is a composite parameter involving the contribution from (i) Henry's law needed for the formation of a site and the dissolution of the species into that site, the formation of the site involves an endothermic contribution and (ii) Langmuir's (hole filling) type sorption mechanism, in which case the site already exists in the polymer matrix and sorption by hole filling gives exothermic heats of sorption. The ΔH_S values are negative for NR suggesting a Langmuir's type sorption. For ENR Henry's law sorption operates as suggested by endothermic heat of sorption. From the values of ΔH_S it is clear that the sorption changes from Langmuir's type to Henry's type with increase in volume fraction of ENR.

TABLE IX Values of ΔH_S (kJ/mol)

Solvent	NR	NR/ENR 70/30	NR/ENR 50/50	NR/ENR 30/70	ENR
Hexane	−0.64	1.23	1.08	1.12	1.03
Heptane	−0.26	0.85	1.65	1.83	1.16
Octane	−0.25	1.0	1.00	1.63	1.05

3.3.5. Interaction parameter

Interaction parameter, χ, has been calculated using the equation [34]

$$\chi = \frac{(\mathrm{d}\phi/\mathrm{d}T)\{\phi/(1-\phi)] + N\ln(1-\phi) + N\phi\}}{\{2\phi(\mathrm{d}\phi/\mathrm{d}T) - \phi^2 N(\mathrm{d}\phi/\mathrm{d}T) - \phi^2/T\}} \tag{14}$$

TABLE X Interaction parameter, χ

Solvent	NR	NR/ENR 70/30	NR/ENR 50/50	NR/ENR 30/70	ENR
Hexane	0.414	0.557	0.632	0.672	0.781
Heptane	0.363	0.392	0.402	0.456	0.535
Octane	0.435	0.586	0.634	0.724	0.812

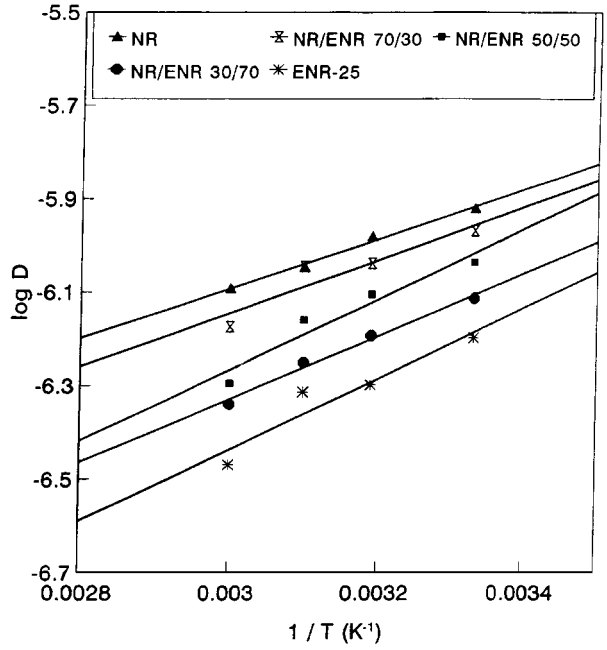

Figure 11 Arrhenius plot of log D vs. $1/T$.

where ϕ is the volume fraction of polymer in the swollen sample and N is calculated from ϕ as

$$N = \frac{(\phi^{2/3}/3 - 2/3)}{(\phi^{1/3} - 2\phi/3)} \tag{15}$$

The χ values are given in Table X. The lowest value is obtained for NR indicating highest interaction of NR with the penetrants. The interaction decrease with increase in volume fraction of ENR and is minimum for ENR. Further, the interaction is found to be maximum for heptane among different solvents in all cases. This further explains the maximum solvent uptake for heptane.

3.4. Determination of the network structure

The investigation of swelling equilibrium can help to elucidate the structure of the polymer network. Flory and Rehner [35] relations were developed for a network deforming affinely, i.e., the components of each chain vector transform linearly with macroscopic deformation and the junction points are assumed to be embedded in the network without fluctuations. Then the molecular weight between crosslinks (M_c) for the affine limit of the model [M_c (aff)] was calculated by the formula [36],

$$M_c\,(\text{aff}) = \frac{\rho V_s \nu_{2c}^{2/3} \nu_{2m}^{1/3} \left(1 - \frac{\mu}{\nu} \nu_{2m}^{1/3}\right)}{-\left(\ln(1 - \nu_{2m}) + \nu_{2m} + \chi \nu_{2m}^2\right)} \tag{16}$$

TABLE XI Comparison of swelling equilibrium properties in hexane

M_c values	NR	NR/ENR 70/30	NR/ENR 50/50	NR/ENR 30/70	ENR
M_c (chem)	4897	4533	4300	4289	3612
M_c (aff)	4540	4188	3941	3648	3310
M_c (ph)	1513	1399	1316	1218	1103

where V_s is the molar volume of the solvent, μ and ν are called the number of effective chains and junctions; ν_{2m}, the polymer volume fraction at swelling equilibrium; ν_{2c}, the polymer volume fraction during crosslinking; and ρ, the polymer density. James and Guth [37] proposed the phantom network model, where the chain may move freely through one another. According to the theory, the molecular weight between crosslinks for the phantom limit of the model [M_c (ph)] was calculated by [36, 38]

$$M_c\,(\text{ph}) = \frac{\left(1 - \frac{2}{\phi}\right) \rho V_s \nu_{2c}^{2/3} \nu_{2m}^{1/3}}{-\left(\ln(1 - \nu_{2m}) + \nu_{2m} + \chi \nu_{2m}^2\right)} \tag{17}$$

where ϕ is the junction functionality.

M_c (aff) and M_c (ph) were compared with M_c (chem) and the values are given in Table XI. It is seen that M_c (chem) values are close to M_c (aff). This suggests that in the highly swollen state, the chains in NR, ENR-25 and the blends deform affinely.

3.5. Mechanism of sorption

In order to understand the mechanism of transport of solvents through NR/ENR blends, the results of sorption experiments were analysed using the following equation [39, 40]

$$\log(Q_t/Q_\infty) = \log k + n \log t \tag{18}$$

where Q_t is the mole per cent sorption at time t and Q_∞ is that at equilibrium, k is a constant which depends upon the structural peculiarities of the system and its interaction with the solvent used. The value of n gives an idea about the mechanism of solvent transport. A value of 0.5 for n suggests a Fickian mode of transport where the rate of polymer chain relaxation is higher than the diffusion rate of the penetrant. When $n = 1$, the diffusion mechanism is said to be non-Fickian at which the chain relaxation is slower than the solvent diffusion. If the value of n falls between 0.5 and 1, the mechanism is said to be anomalous where the polymer chain relaxation rate and solvent diffusion rate are similar. The 'n' values vary from 0.62 to 0.71 for NR suggesting an anomalous sorption behaviour. This may be due to the leaching out of unreacted compounding ingredients from the NR matrix. Sorption-desorption experiments presented in the coming section clearly indicates this. For ENR-25, the values vary from 0.56 to 0.60, suggesting the mechanism to be nearer to Fickian type. This may be due to the decreased diffusion rate of penetrants compared to polymer chain relaxation. The values of n for different blend compositions are in

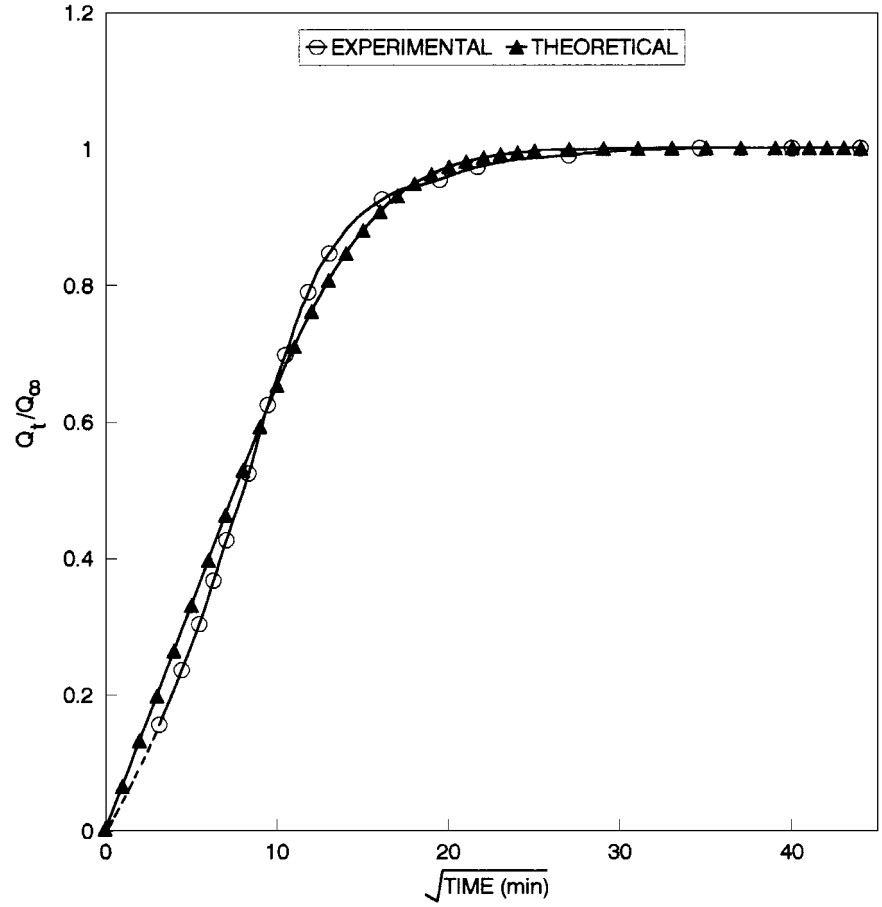

Figure 12 Comparison between theoretical and experimental diffusion profiles for NR/ENR 30/70 in heptane at 27 °C.

between that of NR and ENR which decrease with decreasing volume fraction of ENR. In all cases the value of n decreases with increase of temperature suggesting increased polymer chain relaxation.

The k values are maximum for NR which decreases with volume fraction of ENR and reaches a minimum value for ENR. Further with increase in temperature the values increase showing increased polymer-solvent interaction. Among different polymer-solvent systems, heptane shows the maximum value indicating its increased interaction with the polymer matrix as suggested earlier by the χ values.

Attempt has been made to compare the experimental diffusion curves with the theoretical diffusion profile. The theoretical curves are constructed using the equation, which describes the Fickian diffusion model [41]

$$\frac{Q_t}{Q_\infty} = 1 - \frac{8}{\pi^2}\sum_{n=0}^{\infty}\frac{1}{(2n+1)^2} \cdot \exp[-D(2n+1)^2\pi^2 t/h^2] \qquad (19)$$

Here Q_t and Q_∞ are the mass of solvent uptake at time t, and at equilibrium and h is the initial sample thickness.

The experimentally determined values of diffusion coefficients (D) were substituted in the equation and the theoretical curves are obtained. Comparative study has been made for NR, ENR and their blends. The deviation is found to be maximum for NR and the deviation decreases with the increasing volume fraction of ENR. For ENR the comparison suggests an almost Fickian behaviour. Fig. 12 represent the theoretical and experimental sorption curves of NR/ENR blends.

3.6. Sorption (S)-desorption (D)-resorption (RS)-redesorption (RD)

Sorption process was carried out in polymer samples by the usual method. The swollen samples were then placed in a vacuum oven at constant temperature for desorption measurements. The samples were then subjected to resorption followed by redesorption. Sorption, desorption, resorption and redesorption curves for 70/30 and 50/50 NR/ENR blends are given in Figs 13 and 14 respectively. For desorption experiments, NR has the highest desorption equilibrium value and ENR has the lowest. In the case of blend compositions the maximum desorption equilibrium value is obtained for 70/30 which decreases to 30/70. These observations result from the leaching out of unreacted compounding ingredients from NR matrix. This is further evident from the decrease in desorption equilibrium value as the volume fraction of NR decreases. For ENR the desorption equilibrium is lower than that of sorption equilibrium. This may be due to the ability of the highly crosslinked gel phase in ENR to retain the sorbed solvent molecules. The resorption experiment shows a higher equilibrium uptake for NR resulting from the increase in free volume of NR due to leaching out of additives during sorption-desorption experiments. The redesorption equilibrium does not vary much from

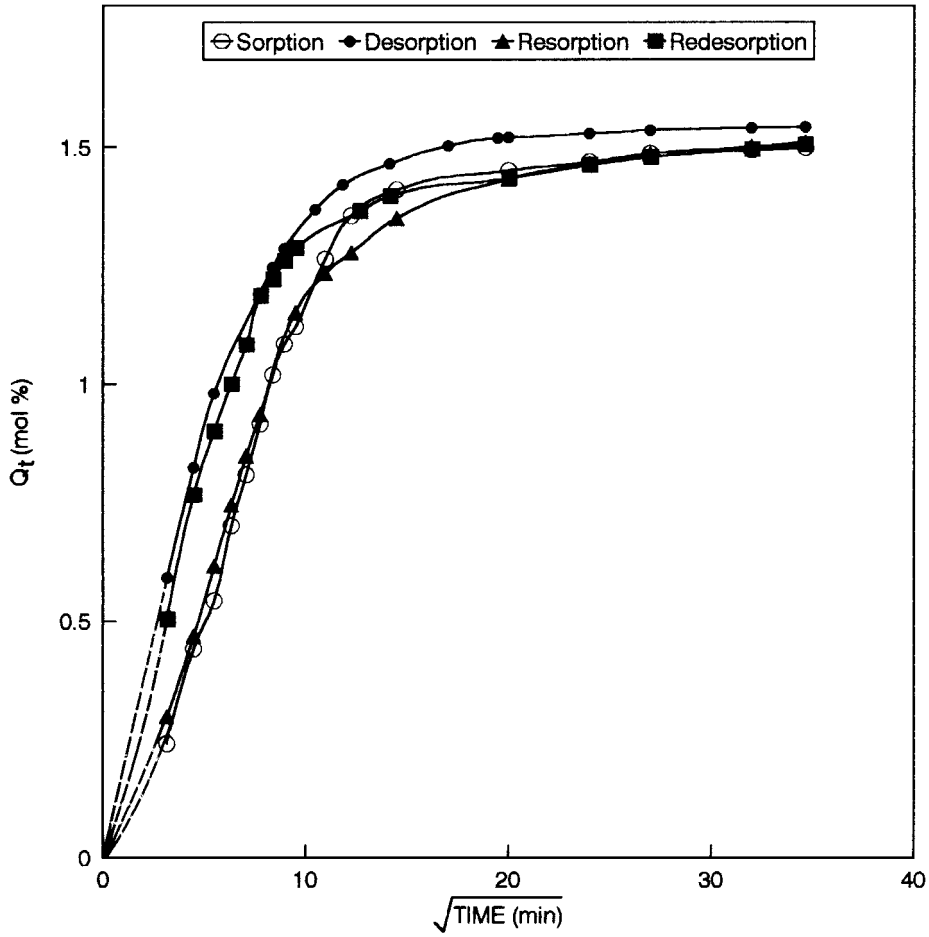

Figure 13 Sorption-desorption-resorption-redesorption plot of NR/ENR 70/30 in hexane at 27 °C.

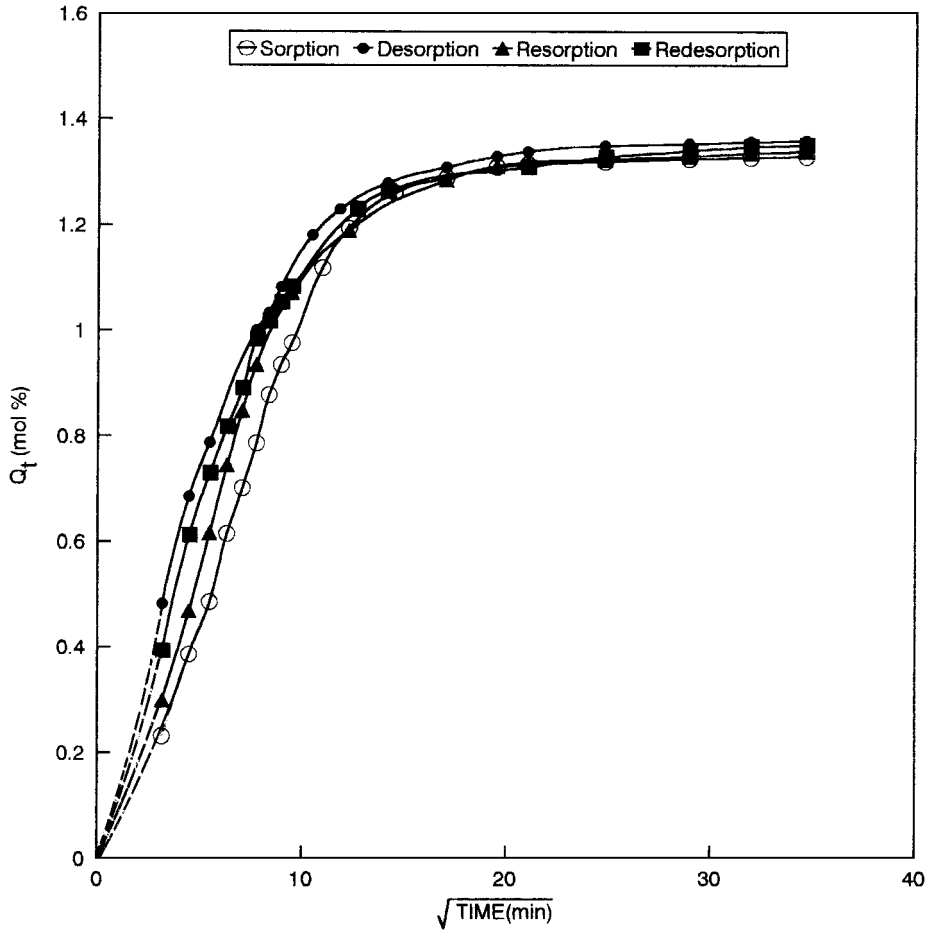

Figure 14 Sorption-desorption-resorption-redesorption plot of NR/ENR 50/50 in hexane at 27 °C.

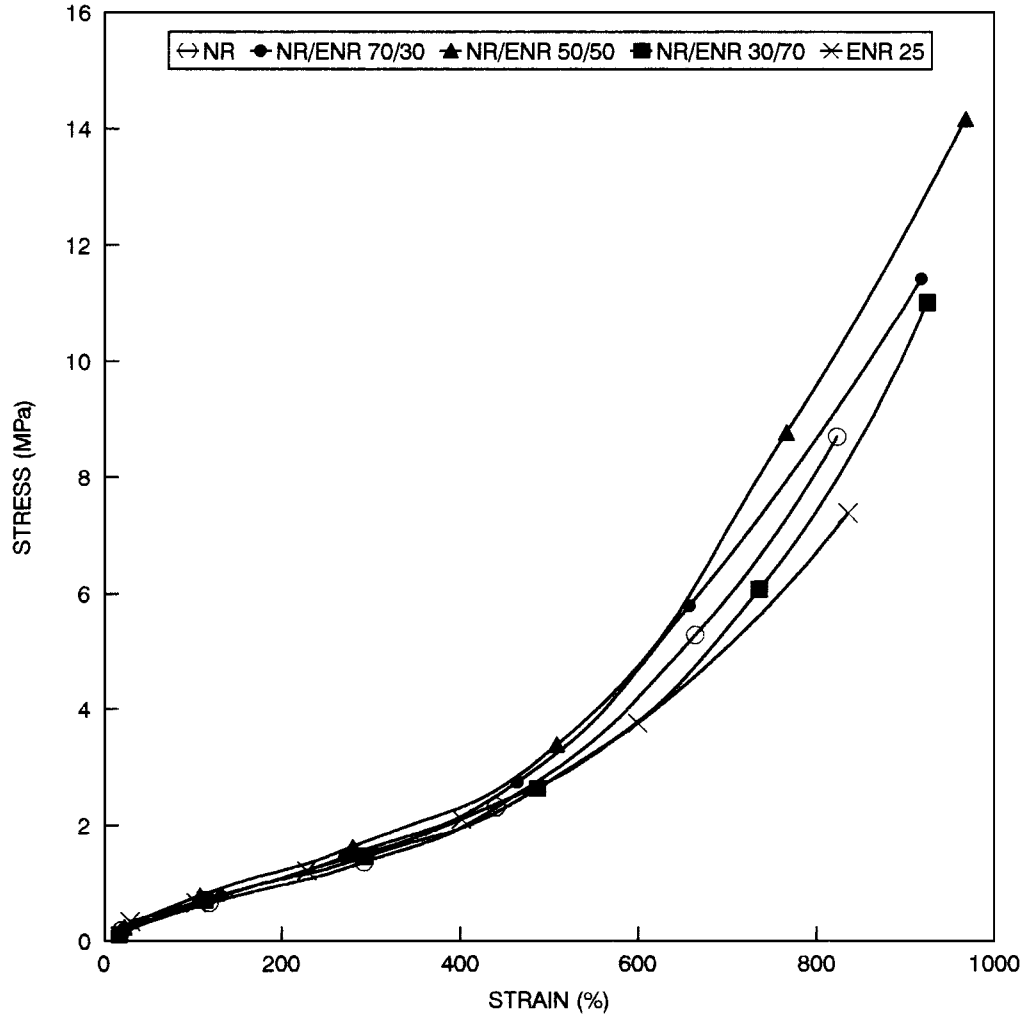

Figure 15 Stress-strain curves of unswollen samples.

resorption equilibrium indicating no further leaching out of additives.

3.7. Mechanical properties

The stress-strain curves of unswollen samples are given in Fig. 15. All the curves show typical elastomeric behaviour. All the blend compositions exhibit superior performance compared to individual components. The stress value attains a maximum for 50/50 composition. This is due to the co-continuous nature of the 50/50 composition. The 70/30 and 30/70 blend show better performance compared to individual components as a result of two main reasons: (1) partial stress transfer is present in these blends (2) the strain crystallisation of NR and ENR.

In the swollen state (Fig. 16) ENR shows higher stress value compared to NR. This is attributed to the extensive swelling of NR which results in reduced strain crystallisation. Here also, blend compositions follow the behaviour of unswollen samples. In general, the stress-strain curves of deswollen samples (Fig. 17) show similar behaviour to those of unswollen samples. But there is an overall increase in magnitude of the maximum stress value. The increase in interchain interaction which results from the leaching out of unreacted compounding ingredients leads to this behaviour.

Mechanical data are presented in Table XII. Tensile strength of unswollen samples is lower for individual components compared to blend compositions which attain a maximum at 50/50 composition. As evident from the morphology, 50/50 composition exhibits a co-continuous structure. With conventional rubber-mixing techniques, equal-volume fractions and equal viscosities of the components will favour co-continuity [42, 43]. Co-continuity implies that an IPN may exist [44]. As reported by Sperling [45] this unique morphology of polymer network can lead to additive properties. From the table, it is clear that tensile strength and modulus values follow the additive or synergistic behaviour. From these it can be inferred that the exceptional properties of 50/50 blend results from an interpenetrating network (IPN) structure. The performance of other blend compositions (70/30 and 30/70) is in between 50/50 and individual components. This may be due to the formation of a partial network structure.

The crosslinking density values of the homopolymers and blends have been calculated using the equation [46]

$$\eta = \frac{F}{2A_0\rho_P RT(\alpha - 1/\alpha^2)} \tag{20}$$

where F is the force required to stretch a specimen to an extension ratio α, A_0, the cross-sectional area of

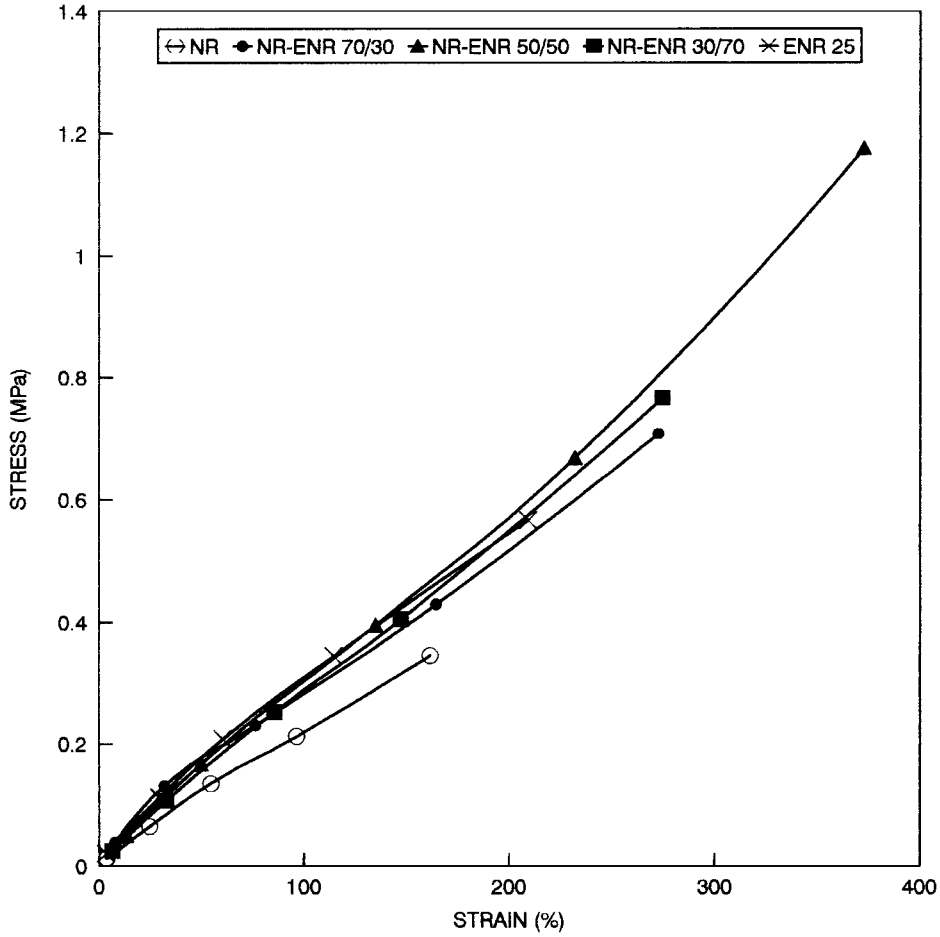

Figure 16 Stress-strain curves of swollen samples.

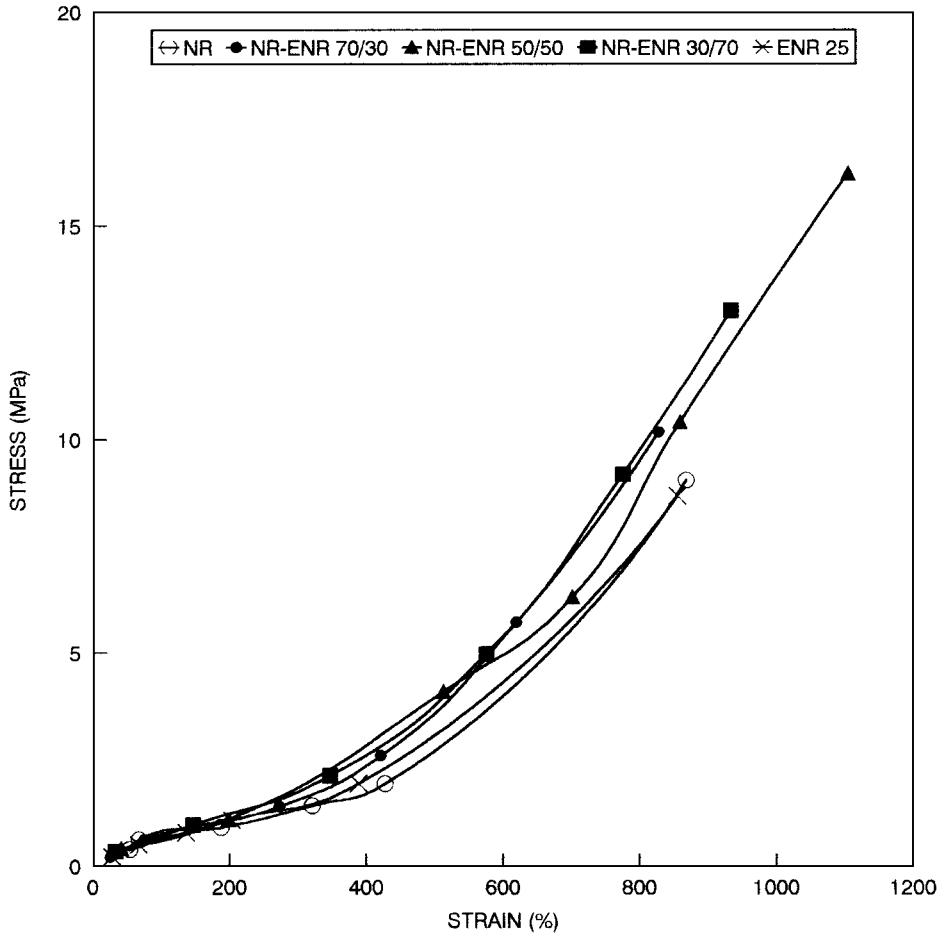

Figure 17 Stress-strain curves of deswollen samples.

TABLE XII Mechanical properties

Sample	System	Tensile Strength (MPa)	EB (%)	Crosslink density ($\nu \times 10^5$) (gmol/m^3)	Young's modulus $\times 10^2$ (MPa)	Secant modulus (MPa)		
						M_{100}	M_{200}	M_{300}
Unswollen	NR	8.69	841	1.94	25.0	0.60	0.96	1.57
	NR/ENR 70/30	11.42	944	2.30	26.2	0.62	1.10	1.67
	NR/ENR 50/50	14.17	978	2.77	33.0	0.72	1.31	1.88
	NR/ENR 30/70	11.00	935	2.27	23.0	0.64	1.09	1.54
	ENR-25	7.38	828	1.61	30.0	0.66	1.19	1.53
Swollen	NR	0.34	194	0.26	1.8	0.21	—	—
	NR/ENR 70/30	0.76	306	0.40	1.3	0.29	0.53	0.79
	NR/ENR 50/50	1.18	406	0.49	1.2	0.28	0.54	0.91
	NR/ENR 30/70	0.79	328	0.39	1.8	0.28	0.53	0.73
	ENR-25	0.56	261	0.34	1.3	0.29	0.54	—
Deswollen	NR	9.05	867	2.24	24.7	0.72	1.03	1.62
	NR/ENR 70/30	12.56	842	2.84	22.7	0.85	1.13	1.77
	NR/ENR 50/50	15.06	1059	2.88	23.7	0.81	1.40	1.89
	NR/ENR 30/70	11.25	833	2.29	23.7	0.67	1.22	1.90
	ENR-25	8.68	854	1.86	31.2	0.76	1.31	1.67

the sample, R, the universal gas constant and T, the absolute temperature. The crosslinking density values are given in Table XII.

This high crosslinking density of 50/50 blend accounts for the superior properties of this composition. The Young's modulus reflects the stress behaviour at low strain while the Secant modulus values represents the behaviour at high strain. A higher Young's modulus value for ENR compared to NR suggest that the initial stretching of ENR requires higher stress but at higher strain ($M300$) the strain crystallisation of NR leads to increased Secant modulus values for NR. Here also blend compositions show higher values.

In swollen state, there is overall reduction in the magnitude of these values. Still the blend compositions exhibit better mechanical properties. Also in deswollen samples, the mechanical properties show improvement compared to unswollen. As explained earlier this may be due to the increase in interchain interaction.

3.7.1. Model fitting

Various composite models such as the parallel model, the series model, the Kerner model and the Kunori model were made use of to study the mechanical behaviour of the blend.

The parallel model (highest-upper-bound model) is given by the equation [47],

$$M = M_1\phi_1 + M_2\phi_2 \tag{21}$$

where M is the mechanical property of the blend and M_1 and M_2 are the mechanical properties of the components 1 and 2, respectively and ϕ_1 and ϕ_2 are the volume fractions of the components 1 and 2, respectively. Here the components are considered to be arranged parallel to one another so that the applied stress elongates each of the components by the same amount.

In the lowest-lower-bound series model, the components are arranged in series with the applied stress and is given by the equation [48],

$$1/M = \phi_1/M_1 + \phi_2/M_2 \tag{22}$$

Kunori *et al.* [49] suggested a model when strong adhesive force exists between the blend components. In this model, the dispersed phase will contribute to the strength of the blend and the equation is

$$\sigma_b = \sigma_m(1 - A_d) + \sigma_d A_d \tag{23}$$

Considering two possible fracture paths in a blend, Equation 23 can be modified as follows depending on whether the fracture is through the interface or through the matrix. When the fracture is through the interface.

$$\sigma_b = \sigma_m\left(1 - \phi_d^{2/3}\right) + \sigma_d\phi_d^{2/3} \tag{24}$$

when the fracture is through the matrix

$$\sigma_b = \sigma_m(1 - \phi_d) + \sigma_d\phi_d \tag{25}$$

where σ_b, σ_m and σ_d are the properties of the blend, matrix phase and dispersed phase respectively and ϕ_d is the volume fraction of the dispersed phase.

The Kerner equation [50] for perfect adhesion is given by

$$E = \left[\frac{\phi_d E_d}{[(7 - 5\nu_m)E_m + (8 - 10\nu_m)E_d]} + \frac{\phi_m}{15(1 - \nu_m)}\Big/\frac{\phi_d E_m}{[(7 - 5\nu_m)E_m + (8 - 10\nu_m)E_d]} + \frac{\phi_m}{15(1 - \nu_m)}\right]E_m \tag{26}$$

where E, E_m and E_d are the respective properties of the blend, continuous phase and dispersed phase, ϕ_d and ϕ_m are the volume fractions of dispersed and continuous phase and ν_m is the Poisson's ratio of the continuous phase.

Fig. 18 shows the theoretical and experimental curves of the tensile strength values of the NR/ENR-25 blend. The theoretical curve based on Equation 24 comes closest to the experimental curve compared to other models.

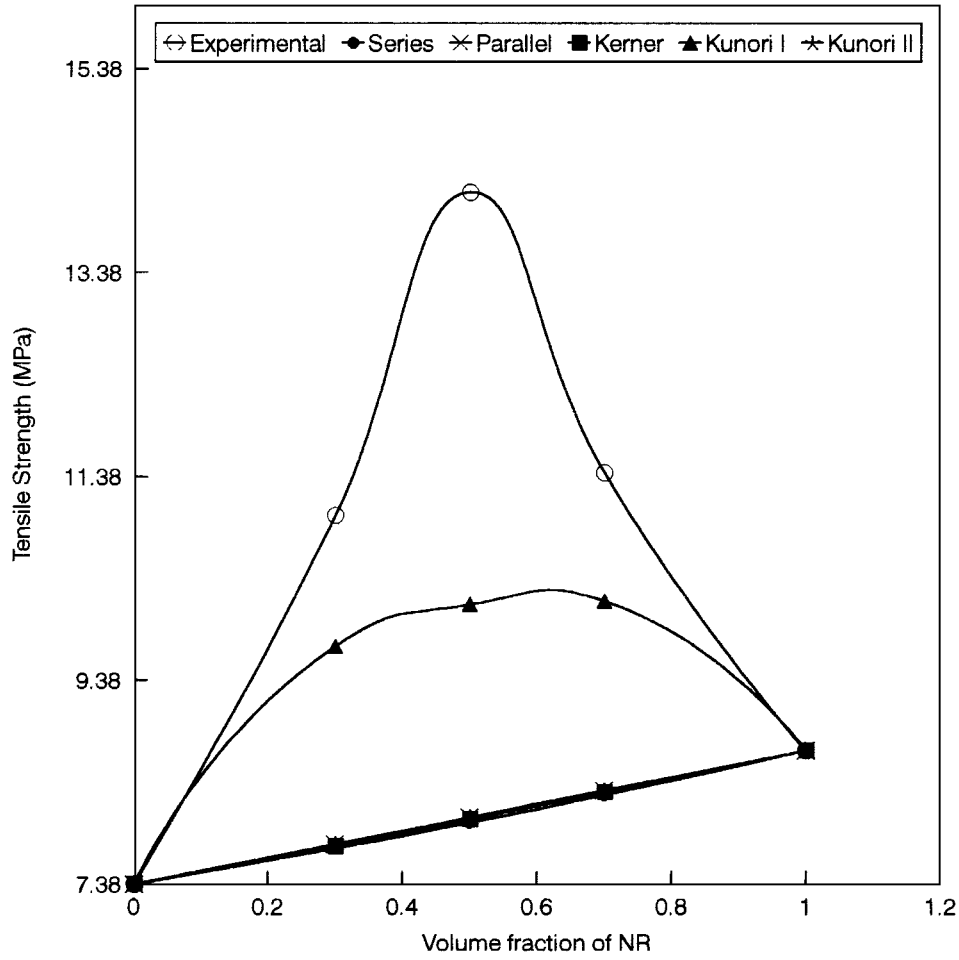

Figure 18 Comparison of experimental tensile strength with theoretical predictions.

So, it may be concluded that the fracture path is through the interface rather than through the matrix. But it was found that the experimental data are above the theoretical values in all cases. The deviation of experimental values from theoretical values are more pronounced for NR/ENR 50/50 composition. This may be because of the fact that both NR and ENR-25 phases have an interpenetrating co-continuous morphology at 50/50 composition.

4. Conclusion

Blend morphology, transport behaviour and mechanical properties of natural rubber, epoxidised natural rubber and their blends have been established. The heterogeneous nature of the blend under consideration is evident from the SEM studies. The 50/50 composition shows a co-continuous morphology. Further the different transport parameters establish the heterophase nature of the blend. Diffusion coefficient, rate constant and permeation and sorption coefficients are intermediate to those of the components. Further, interaction parameter also shows the same trend. Enthalpy of sorption shows that Langmuir's type sorption mechanism operates in natural rubber which changes to Henry's law type sorption with increase in volume fraction of ENR. Comparison with theory establishes that the mechanism of diffusion to be anomalous for NR. The deviation from theoretical prediction decreases with increase in volume fraction of ENR and finally the experimental diffusion profile approaches to theoretical predication for ENR. There is marked improvement in mechanical properties of all blend compositions compared to that of the components. The exceptional performance of 50/50 composition may be the result of the formation of an interpenetrating type network. In all cases, the deswollen samples show increased mechanical properties compared to unswollen samples. Improved polymer chain interaction resulting from the leaching out of additives may be the reason for this observation. Further, experiments are in progress on the use of these membranes for the separation of liquid mixtures.

Acknowledgement

One of the authors, T. Johnson is grateful to UGC for the award of Junior Research Fellowship.

References

1. R. B. MESROBIAN and C. J. AMMONDSON, *US Patent* No. 3, **093** (1963) 255.
2. D. M. CATES and H. J. WHITE JR., *J. Polym. Sci.* **20** (1956) 181.
3. *Idem., ibid.* **20** (1956) 155.
4. *Idem., ibid.* **21** (1956) 125.
5. W. N. KING, D. L. HOENSCHEMEYER and C. W. SALTONSTALL JR., in "Reverse Osmosis Membrane Research" (Edited by H. K. Lonsdale and H. E. Podall) (Plenum Press, New York, 1972) p. 131.
6. E. SHCHORI and J. JAGUR-GRODZINSKI, *J. Appl. Polym. Sci.* **20** (1976) 773.

7. T. M. AMINABHAVI and H. T. S. PHAYDE, *ibid.* **57** (1995) 1491.
8. *Idem., Eur. Polym. J.* **32** (1996) 1117.
9. C. H. M. JACQUES, H. B. HOPFENBERG and V. J. STANNET, *Polym. Eng. Sci.* **13** (1973) 81.
10. C. H. M. JACQUES and H. B. HOPFENBERG, *ibid.* **14** (1974) 449.
11. H. B. HOPFENBERG, V. J. STANNET and G. M. FOLK, *ibid.* **15** (1975) 261.
12. H. P. GREGOR, H. JACOBSON, R. C. SHAIR and D. M. WETSTONE, *J. Phys. Chem.* **61** (1957) 141.
13. H. P. GREGOR and D. M. WETSTONE, *ibid.* **61** (1957) 147.
14. D. M. WETSTONE and H. P. GREGOR, *ibid.* **61** (1957) 151.
15. J. BARRER, *Rubber Chem. Technol.* **28** (1955) 814.
16. G. GILLBERG, L. C. SAWYER and A. L. PROMISLOW, *J. Appl. Polym. Sci.* **28** (1983) 3723.
17. K. FUJIMOTO, T. NISHI and T. OKAMATO, *Int. Polym. Sci. Technol.* **8**(8) (1981) T/30.
18. J. E. DAVEY and M. J. R. LOADMAN, *Br. Polym. J.* **16** (1984) 134.
19. D. R. BURFIELD, K. K. LIM, K. S. LAW and S. NG, *Polymer* **25**(7) (1984) 995.
20. C. M. ROLAND and G. G. A. BÖHM, "ACS Natl. Meeting" (Washington, DC, 1983).
21. N. TOKITA, *Rubber Chem. Technol.* **50** (1977) 293.
22. A. D. T. GORTON and T. D. PENDLE, *NR Technology* **12** (1981) 1.
23. A. K. BHOWMICK and H. L. STEPHENS, "Handbook of Elastomers" (Marcel Dekker, Inc., 1988).
24. P. E. FROETHING, D. M. KOENHEN, A. BANTJES and C. A. SMOLDERS, *Polymer* **17** (1976) 835.
25. Y. M. LEE, D. BOURGEOIS and G. BELFORT, *J. Membr. Sci.* **44** (1989) 161.
26. G. W. R. DAVISON and N. A. PEPPAS, *J. Controlled Release* **3** (1986) 243.
27. R. W. KORSMEYER, E. W. MEERWALL and N. A. PEPPAS, *J. Polym. Sci., Polym. Phys. Edn.* **24** (1986) 409.
28. J. S. CRANK, "The Mathematics of Diffusion," 2nd ed. (Clarendon Press, Oxford, 1975).
29. S. B. HAROGOPPAD and T. M. AMINABHAVI, *Macromolecules* **24** (1991) 2598.
30. R. S. KHINNAVAR and T. M. AMINABHAVI, *J. Appl. Polym. Sci.* **42** (1991) 2321.
31. G. R. GARBARINI, R. F. EATON, T. K. KWEI and A. V. TOBOLSKY, *J. Chem. Educ.* **48** (1971) 226.
32. H. SCHOTT, *J. Macromol. Sci. Phys.* **B31** (1992) 1.
33. T. M. AMINABHAVI and R. S. MUNNOLI, *J. Hazard Mater.* **38** (1994) 223.
34. U. S. AITHAL, T. M. AMINABHAVI and P. E. CASSIDY, in "Barrier Polymers and Structures" (edited by W. J. Koros (Am. Soc. Symp. Ser. 423), 197th National Meeting (Dallas, TX, Am. Chem. Soc., Washington, DC, 1989) p. 351.
35. P. J. FLORY, "Principles of Polymer Chemistry" (Cornell University Press, Ithaca, 1953).
36. L. R. G. TRELOAR, "The Physics of Rubber Elasticity" (Clarendon Press, Oxford, 1975).
37. H. M. JAMES and E. GUTH, *J. Chem. Phys.* **15** (1947) 669.
38. J. E. MARK and B. ERMAN, "Rubberlike Elasticity, a Molecular Primer" (Wiley, New York, 1988).
39. J. S. CHIOU and D. R. PAUL, *Polym. Eng. Sci.* **26** (1986) 1218.
40. L. M. LUCHT and N. A. PEPPAS, *J. Appl. Polym. Sci.* **33** (1987) 1557.
41. A. N. GENT and R. H. TOBIAS, *J. Polym. Sci. Polym. Phys Edn.* **20** (1982) 2317.
42. G. N. AVGEROPOULOS, F. C. WEISSERT, P. H. BIDDISON and G. G. A. BÖHM, *Rubber Chem. Technol.* **49** (1976) 93.
43. W. P. GERGEN, S. DAVISON and R. H. LUTZ, "Rubber Div. Meeting" (ACS, Los Angeles, Paper No. 2).
44. L. H. SPERLING and D. W. FRIEDMAN, *J. Polym. Sci.* **A2**(7) (1969) 425.
45. L. H. SPERLING, "Interpenetrating Polymer Networks and Related Materials" (Plenum Press, New York, 1981).
46. H. F. MARK, N. M. BIKALES, C. G. OVERBERGE and G. MENGES, "Encyclopaedia of Polymer Science and Engineering," Vol. 4 (John Wiley and Sons, 1986) p. 356.
47. S. GEORGE, L. PRASANNAKUMARI, P. KOSHY, K. T. VARUGHESE and S. THOMAS, *Mater. Lett.* **26** (1996) 51.
48. S. GEORGE, R. JOSEPH, K. T. VARUGHESE and S. THOMAS, *Polymer* **36**(23) (1995) 4405.
49. T. KUNORI and P. H. GEIL, *J. Macromol. Sci. Phys. B* **18**(1) (1980) 135.
50. E. H. KERNER, *Proc. Phys. Soc.* **69B** (1956) 808.

Received 16 December 1997
and accepted 13 January 1999